JOURNAL OF MATERIALS SCIENCE 27 (1992) 3389–3394

Critical strength criteria for DB/SPF processing of Al–Li 8090 alloy

D. V. DUNFORD, P. G. PARTRIDGE
Materials and Structures Department, DRA Aerospace Division, Royal Aerospace Establishment, Farnborough GU14 6TD, UK

Peel strengths are reported for solid state or transient liquid-phase diffusion-bonded (DB) joints between aluminium–lithium 8090 alloy sheets. The joints were tested under superplastic forming (SPF) conditions at 530 °C and with a progressively increasing peel angle, θ, in the range 0°–60°. The sheet deformed superplastically with or without peel fracture of the joints. A deformation model is proposed which predicts a critical combination of peel strength and superplastic flow stress for DB/SPF processing of the 8090 alloy and indicates peel fracture will occur when sheet thicknesses exceed 2 and 0.8 mm in solid state and transient liquid-phase diffusion-bonded joints, respectively.

1. Introduction

Superplastic forming (SPF) is an established process for thin titanium and aluminium alloy sheet [1, 2]. For titanium alloys this process has been combined with diffusion bonding (DB/SPF) to produce multiple sheet aerospace structures at lower cost [3, 4]. A similar production route for aluminium alloy structures has been limited by the DB joints. It is much more difficult to obtain reproducible high-strength bonded joints between aluminium alloys because of their stable surface oxide films [5]. However surface films on lithium containing aluminium alloys are less stable [6] and high-strength solid state and transient liquid-phase bonds have been produced between Al–Li 8090 alloy sheets [7–9]. The shear strength at room temperature and the 90° "T" peel strength at room and at the superplastic forming temperature (530 °C) have been reported for bonded joints in this alloy [7, 9–11]. It was concluded that at the SPF temperature 90° peel fracture would occur before superplastic strain in the sheet unless the sheet was very thin (< 1 mm) [11].

In practice, the peel angle, θ, is usually much less than 90°, which may increase the force required for peel fracture above that required for SPF. In addition, the progressive reduction in sheet thickness with increasing superplastic strain leads to a corresponding lower force for SPF which favours superplastic deformation rather than peel fracture. The relationship between peel angle and the forces for peel and SPF have been investigated using a bonded 8090 sheet test piece that simulates DB/SPF processing. The results obtained are described in this paper and used to predict the dominant deformation mode and optimum sheet thickness during DB/SPF processing of 8090 alloy.

2. Experimental procedure

Aluminium–lithium alloy 8090 sheets (composition (wt %) of Al–2.5Li–1.3Cu–0.6Mg–0.12Zr–0.1Fe–0.05Si) 1.6 and 4 mm thick, were mechanically polished and degreased prior to DB either in the solid state without interlayers, or via a transient liquid phase (TLP) using a thin ~ 10 μm copper interlayer (8 μm foil sandwiched between copper sputter-coated sheet surfaces). DB was carried out in a vacuum hot press at 550 °C for 2 h, or 560 °C for 4 h, under a pressure of 0.75 MPa.

A bonded test piece with a variable peel angle, θ, was used to simulate the superplastic forming process. Two sheets (70 mm × 40 mm and 70 mm × 18 mm) were bonded and in the centre of the large sheet a section 20 mm × 18 mm wide was machined to the depth of the bond plane (at B in Fig. 1a). Span thicknesses for the smaller sheet of 0.8–2.0 mm were obtained by machining the whole of the upper surface of the sheet. Plates on each side of the small sheet were used to bolt the test piece to two Al–Li alloy (8090) blocks (D in Fig. 1c), and a 4 mm diameter pin inserted beneath the span midpoint prior to loading in three-point bend as shown in Fig. 1b and c.

Tests were carried out under SPF conditions at 530 °C and at a strain rate in the span (A in Fig. 1a) equivalent to $3 \times 10^{-4}\ s^{-1}$ when θ = 45°.

The effect of SPF strain on the microstructure of solid state diffusion bonds was studied using a bonded specimen (Fig. 2) pulled in tension at 530 °C under SPF conditions.

3. Results

3.1. Peel tests

In solid state DB test pieces the thin sheet was bent to a maximum angle, θ, of ~ 60° without peel fracture at the DB interface (Fig. 1); fracture eventually occurred after thinning and cavitation in the sheet near the loading pin. The minimum initial sheet thickness used (~ 0.8 mm) gave rise to the greatest superplastic

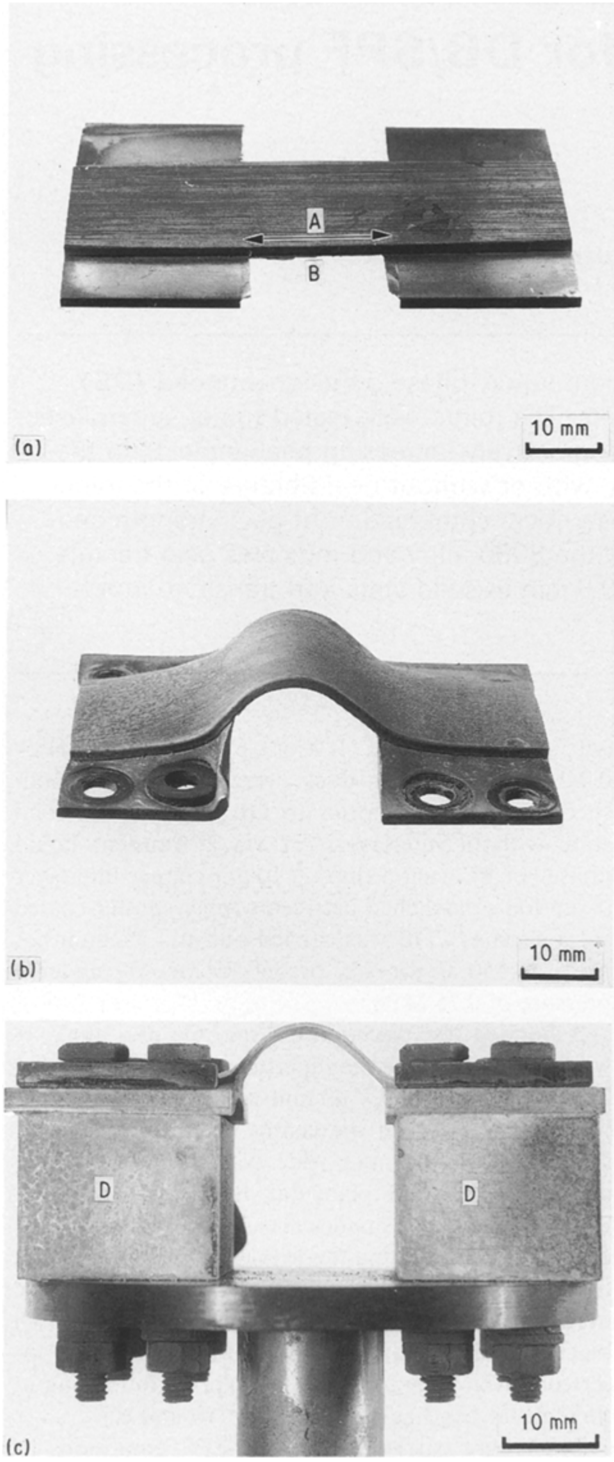

Figure 1 Peel test piece: (a) as-bonded, (b, c) after peel testing.

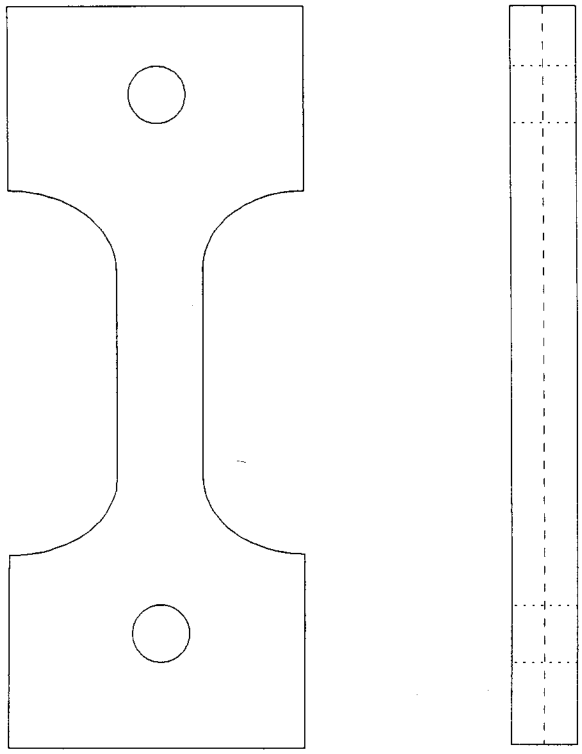

Figure 2 Schematic diagram of bonded joint in the tensile test piece. (– – – – –) Bondline.

thickness strain ($\varepsilon = \sim 0.6$) and to the greatest stress in the sheet. The stress in the sheet (Table I) also caused bending of the thicker sheet (Fig. 3a). After bending to a similar angle, two TLP DB test pieces showed peel fracture at the DB interface (Fig. 3b) and the sheet thickness strain was less. In a third TLP DB test piece, thinning was less uniform and led to fracture near the pin at a lower load but without peel fracture.

The forces acting on the bond are shown in Fig. 4. The resolved normal (peel) force, F_n, is given by the equation

$$F_n = F_a \sin\theta \tag{1}$$

where F_a is the applied force in the sheet, and θ is the angle between sheet and bond plane. If $\theta = 90°$, $F_n = F_a$ and when peel fracture occurs the peel strength is equal to F_n/w (N mm^{-1}), where w is the bond and sheet width. Values for F_a and F_n/w obtained in the present tests are listed in Table I. In solid state DB joints, the maximum F_n/w values were lower than $\sim 5\,\mathrm{N\,m^{-1}}$ required for steady state peel [9–11]. For TLP DB test pieces, F_n/w values were equal to, or higher than, the values for steady state peel strength [10, 11], which is consistent with the observed fracture behaviour.

Previous results for 90° "T" peel test pieces [10, 11] also indicated solid state bonded joints had higher peel strengths than TLP DB joints tested under similar SPF conditions. There was no effect of bond thermal cycle on test data.

3.2. Effect of superplastic strain on the microstructure of solid state diffusion-bonded joints

After a bond thermal cycle, the planar grain boundary at the bond interface appeared unaffected (A–A in Fig. 5a). However, in the tensile test piece (Fig. 2) deformed superplastically to a thickness true strain of ~ 0.6, the planar bond interface was replaced by a larger recrystallized grain microstructure containing cavities (Fig. 5b), which is characteristic of sheet

TABLE I Forces acting on diffusion-bonded joint and corresponding tensile stresses in the sheet test piece arms at 530 °C

Bond type	Bonding cycle[a]	Span thickness, t (mm)	Applied pin load (N)	Force acting in sheet, F_a (N)	Final bend angle, θ (deg)	Resolved normal peel strength, F_n/w ($\mathrm{N\,mm^{-1}}$)	Stress in sheet (MPa)
Solid state	A	0.76	86	43	61	2.1	4.6
	A	0.82	98	49	61	2.4	4.5
	A	1.43	143	71.5	58	3.3	3.8
	B	1.47	146	73	54	3.2	3.6
	A	2	188	94	60	4.5	3.7
TLP	A	1.4	175	87.5	50–53	3.6–3.7[b]	4.2
	B	1.4	155	77.5	56–58	3.6–3.7[b]	3.8
	B	1.4	127	63.5	55	2.9	3.5

[a]A = 4 h/560 °C/0.75 MPa, B = 2 h/550 °C/0.75 MPa.
[b]Peel at DB interface, remaining test pieces fractured in sheet near loading pin.

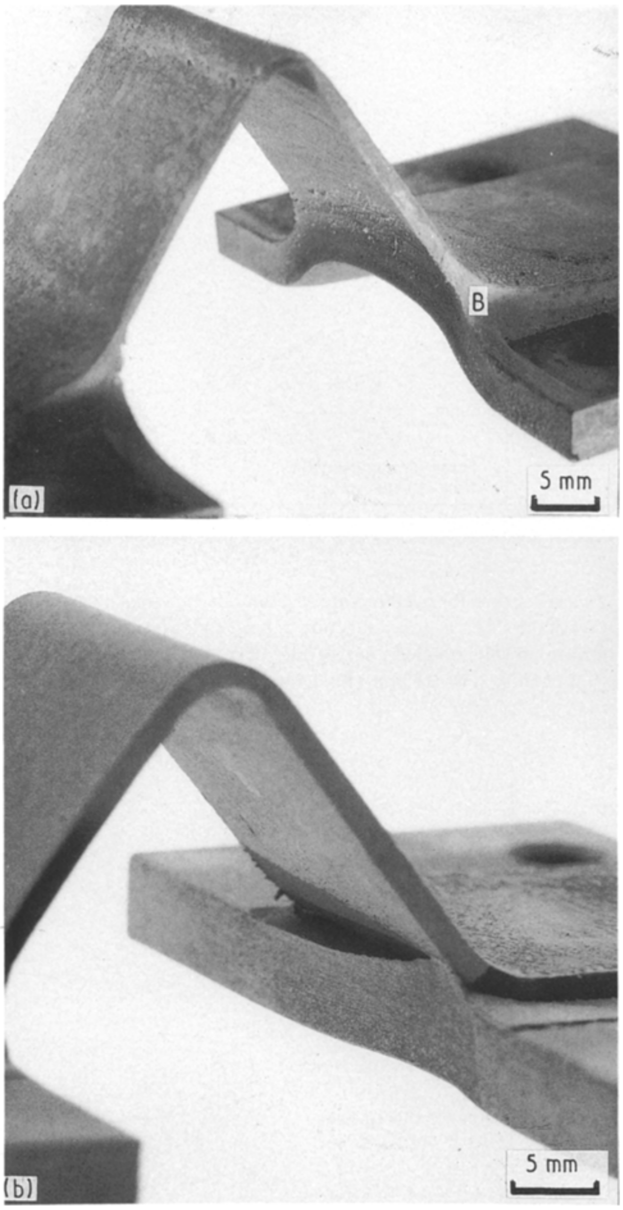

Figure 3 View of test piece after testing: (a) solid state bonded joint, (b) transient liquid-phase bonded joint.

superplastically deformed without back pressure [12]. Similarly in the solid state DB peel test piece the bond interface in the bend region (B in Fig. 3a) also became non-planar.

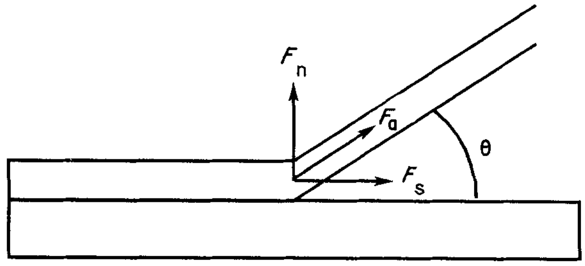

Figure 4 Schematic diagram of forces in a loaded joint.

4. Discussion

The above peel test data at 530 °C suggest that for solid state DB test pieces in sheet thicknesses 0.8–2 mm thick, superplastic deformation to angles of $\sim 60°$ is possible without peel fracture of the DB interface. Some peel fractures occurred in TLP DB test pieces with 1.4 mm thick sheet, suggesting a lower sheet thickness is required to avoid peel and confirming the inherent lower peel strength for this type of bond. Superplastic strain caused the bond interface in the solid state bond to become non-planar, and this is expected to increase the bond strength [7, 13].

These results allow the prediction of the forces for peel and superplastic deformation, and possibly the prediction of the dominant deformation mode during DB/SPF. Consider the deformation of a bonded test piece, shown schematically in Fig. 6. For a fixed test piece and bond width, w, and constant bond strength, the applied force, F_a (equal to half the load on the pin), required to cause peel fracture will be denoted F_p and is related to the angle θ by Equation 1; note this force is not dependent on sheet thickness but only on bond width. A solid state bonded 90° "T" peel test piece in a 1.6 mm thick, 18 mm wide 8090 sheet had a peel strength of $\sim 5\ \mathrm{N\,mm^{-1}}$ [11], i.e. $\theta = 90°$ and $F_n = F_p = 5 \times 18 = 90$ N. Using this value of F_n and Equation 1, values of F_p were calculated and are plotted versus θ in Fig. 7; the corresponding curve for a TLP joint is shown in Fig. 8. These curves, which apply to all sheet thicknesses, show that the force required to peel the bond decreases with increase in θ.

During deformation under superplastic conditions the reduction in sheet thickness leads to a correspond-

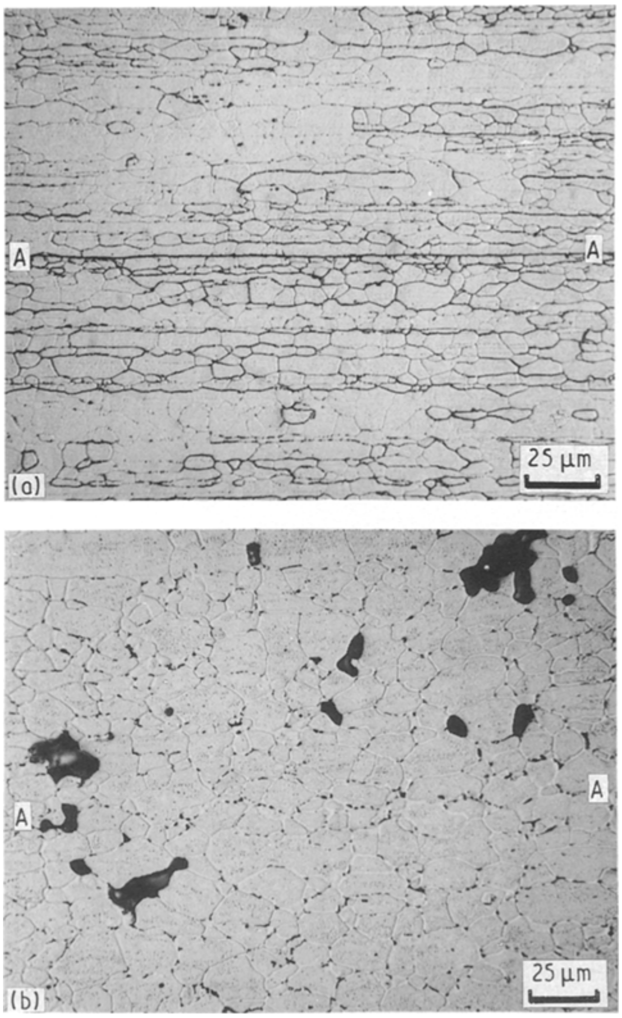

Figure 5 Microstructure of solid state bonded joint: (a) after thermal cycling, (b) after superplastic deformation in the tensile test piece.

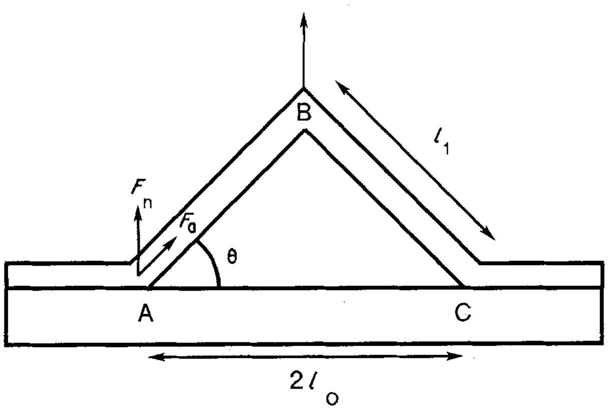

Figure 6 Schematic diagram of dimensions and forces for the peel test piece.

ing reduction in the applied force required to cause superplastic deformation of the sheet, i.e. $F_a = F_{spf}$. An approximate value for F_{spf} can be obtained assuming the volume and width of the sheet remain unchanged and the strain in the sheet is uniform. From Fig. 6 the sheet length AC ($2l_0$) becomes ABC ($2l_1$) and the sheet thickness reduces from t_0 to t_1, i.e. $V = l_0 w_0 t_0 = l_1 w_0 t_1$, $\cos\theta = l_0/l_1$ and the sheet thickness is related to θ by

$$t_1 = t_0 \cos\theta \tag{2}$$

Because the force $F_{spf} = \sigma_{spf} w_0 t_1$, where σ_{spf} is the superplastic flow stress for 8090 alloy, then

$$F_{spf} = \sigma_{spf} w_0 t_0 \cos\theta \tag{3}$$

Unlike F_p, F_{spf} depends on sheet width and thickness. In the test piece used assuming $w_0 = 18$ mm, $t_0 = 1.4$ mm and $\sigma_{spf} = 5$ MPa [14], $F_{spf} = 154\cos\theta$. Thus as the angle θ increases in Fig. 6, the force, F_{spf}, required to cause superplastic deformation of the sheet decreases, as shown for sheet thicknesses in the range 0.8–2 mm in Figs 7 and 8 for solid state and TLP-bonded joints, respectively.

When $F_p > F_{spf}$, superplastic deformation is predicted to occur in the sheet without peel fracture. The

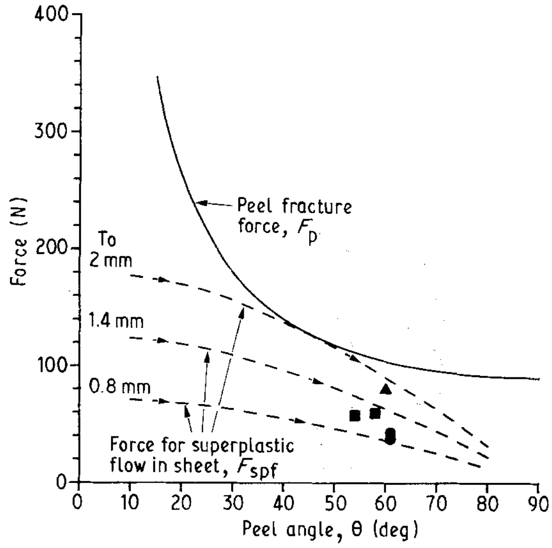

Figure 7 Force for peel fracture, F_p, and for superplastic deformation of the sheet, F_{spf}, as a function of peel angle and sheet thickness for a solid state bonded joint, at 530 °C, $\sigma_{spf} = 5$ MPa, sheet width = 18 mm. t_0: (●) 0.8 mm, (■) 1.4 mm, (▲) 2 mm.

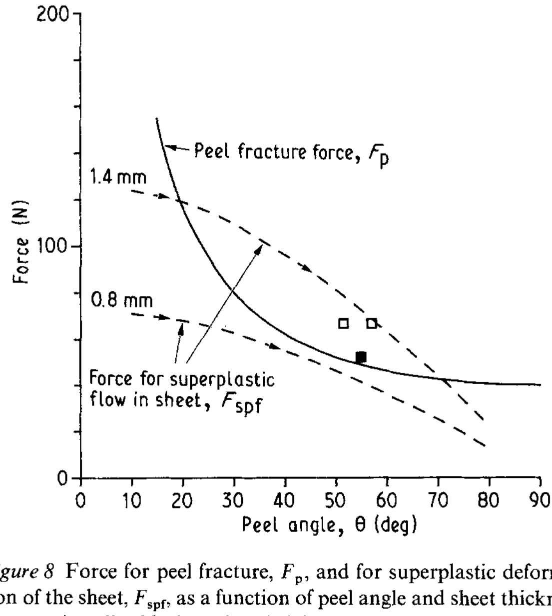

Figure 8 Force for peel fracture, F_p, and for superplastic deformation of the sheet, F_{spf}, as a function of peel angle and sheet thickness for transient liquid-phase bonded joint, at 530 °C, $\sigma_{spf} = 5$ MPa, sheet width = 18 mm, $t_0 = 1.4$ mm. (□) Peel failure, (■) tensile failure.

curves for F_p and F_{spf} are compared in Figs 7 and 8. The experimental data for the solid state joints are in good agreement with the F_{spf} curves which predict only superplastic deformation of the sheet (Fig. 7). The predicted maximum sheet thickness that can be used without causing peel is 2 mm, with the forces for peel and SPF equal (i.e. the ratio $F_{spf}/F_p = 1$) at $\theta = 45°$.

The predicted force curves for TLP joints are compared with the test results in Fig. 8. For two specimens the ratio $F_{spf}/F_p > 1$ and failure was by peel in agreement with the predicted curve. However, in one specimen the strain in the sheet was less uniform and cavitation and tension failure occurred in the sheet with $F_{spf} \sim F_p$. The predicted maximum sheet thickness that can be used without causing peel in a TLP joint is ~ 0.8 mm.

If with increasing angle θ or increasing sheet thickness, the F_{spf} curve cuts the F_p curve (at the ratio $F_{spf}/F_p = 1$), a transition occurs from entirely superplastic deformation of the sheet (when $F_{spf}/F_p < 1$) to concomitant superplastic deformation and peel fracture (when $F_{spf} > F_p$). Peel fracture will become more dominant as the ratio F_{spf}/F_p increases above unity. Values for this ratio are plotted for 2.5 mm sheet in the solid state bonded joint in Fig. 9. The curve shows that angles less than 30° will be required to avoid peel fracture. However, it is apparent that the ratio increases and then decreases as θ increases and, in many cases, some peel fracture may be acceptable in order to obtain the required angle θ.

In practice with multiple DB/SPF sheet structures, θ may be fixed by the design and it is more important to obtain a particular sheet thickness after SPF. The horizontal lines in Fig. 10 represent constant sheet thickness contours. These enable the determination of the initial sheet thickness, t_0, and angle θ required for a given final sheet thickness, t_1, after forming. For example from Fig. 10, for a final sheet thickness of $t_1 = 1.4$ mm, initial sheet thicknesses of 1.7, 2 and 2.5 mm could be used with angles in the range 35°–55° and with the largest angle involving some

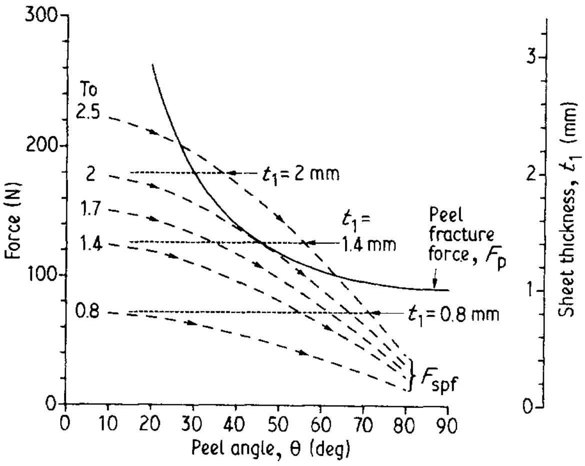

Figure 10 Constant sheet thickness contours superimposed on the force versus peel angle diagram (see text). Solid state bond at 530 °C. (– – –) F_{spf} or t_1, (- - - -) constant thickness contours.

peel fracture. Alternatively, an angle of 45° could be obtained without peel fracture using a sheet thickness of 2 mm.

More accurate predictions will require many other factors to be considered. For example, the geometry of the joint (bend radii and joint stiffness [10, 11]) and loading rate [11] affect the peel fracture force, F_p. The values for θ and F_{spf} will depend on the uniformity of the superplastic strain in the sheet which, in turn, depends on the superplastic flow stress given by the equation [15]

$$\sigma_{spf} = k\dot{\varepsilon}^n \dot{\varepsilon}^m$$

where k is a constant, and ε^n and ε^m describe the strain hardening and strain rate dependence, respectively. Superplastic flow stresses reported for Al–Li 8090 alloy vary between 4 and 8 MPa [14]. With the current bond strengths and with more precise values for the above variables, it should be possible to process 8090 Al–Li alloy by DB/SPF.

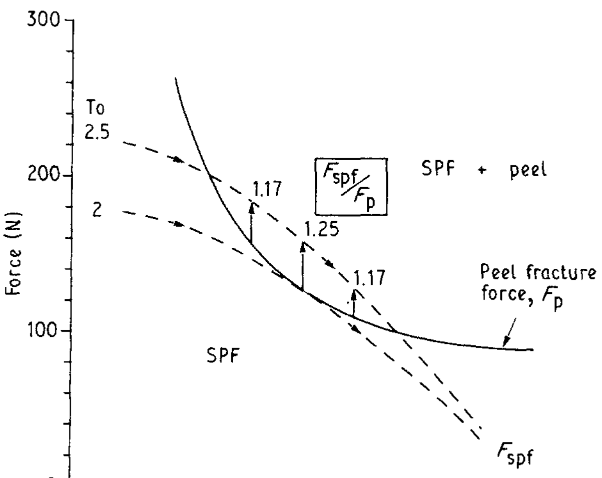

Figure 9 Force for peel fracture, F_p, and for superplastic deformation of the sheet, F_{spf}, as a function of peel angle and sheet thickness for a solid state bonded joint with a ratio $F_{spf}/F_p > 1$.

5. Conclusion

Solid state or transient liquid-phase diffusion-bonded joints between Al–Li 8090 alloy sheets were deformed superplastically with or without peel fracture of the joints. A simple deformation model has been used to relate the peel angle, θ, and the forces for peel fracture and superplastic flow and to predict the sheet thickness after SPF for a given initial sheet thickness. The model predicts a critical combination of peel strength and superplastic flow stress for DB/SPF processing of 8090 alloy and indicates peel fracture will occur when sheet thicknesses exceed 2 mm and 0.8 mm in solid state and transient liquid phase diffusion-bonded joints, respectively.

Acknowledgement

The authors are grateful to Dr D. S. McDarmaid for many helpful discussions. This paper is published with permission of the Controller, HMSO, holder of Crown Copyright.

References

1. D. STEPHEN, "Designing with Titanium" (Institute of Metals, 1986), pp. 252.
2. A. J. BARNES, in "Superplasticity in Aerospace", edited by H. C. Heikkenen and T. R. McNelley (TMS, Pennsylvania, 1988) pp. 301–13.
3. H. E. FRIEDRICH and P-J. WINKLER, in "Superplasticity in Advanced Materials", edited by S. Hori, M. Tokizane and N. Furushiro (Jpn. Society for Research on Superplasticity, 1991) pp. 601–610.
4. M. H. MANSBRIDGE, 22nd International SAMPE Technical Conference (SAMPE, 1990) p. 224.
5. N. RIDLEY, J. PILLING, A. TEKEN and Z. X. GUO, in "Diffusion Bonding", edited by R. Pearce (SIS, Cranfield, Bedford, UK, 1987) pp. 129–42.
6. P. G. PARTRIDGE, *Int. Mater. Rev.* **35** (1990) 37.
7. D. V. DUNFORD and P. G. PARTRIDGE, *J. Mater. Sci.* **25** (1990) 4957.
8. G. A. MAHON, R. KEYTE, N. C. PARSON and R. A. RICKS, in "Superplasticity in Metals. Ceramics and Intermetallics", Materials Research Society, Vol. 196. edited by M. J. Mayo, M. Kobayashi and J. Wadsworth (Materials Research Society, PA, 1990) pp. 155.
9. P. G. PARTRIDGE and D. V. DUNFORD, *ibid.* p. 143.
10. D. V. DUNFORD and P. G. PARTRIDGE, in "Superplasticity in Advanced Materials", edited by S. Hori, M. Tokizane and N. Furushiro (Jpn. Society for Research on Superplasticity, 1991) pp. 795–800.
11. *Idem, J. Mater. Sci* (1992) in press.
12. R. A. RICKS and P-J. WINKLER, in "Superplasticity and Superplastic Forming", edited by C. H. Hamilton and N. E. Paton (TMS, PA, 1989) pp. 377–81.
13. D. V. DUNFORD and P. G. PARTRIDGE, *J. Mater. Sci.* **26** (1991) 2625.
14. R. GRIMES and R. G. BUTLER, in "Superplasticity in Aerospace", edited by H. C. Heikkenen and T. R. McNelley (TMS, PA, 1988) pp. 97–113.
15. C. H. HAMILTON, Nato Agard Lecture Series, "Superplasticity", LS168 (1989) p. 2-1.

Received 8 August
and accepted 10 September 1991